Bacteriophage φMAM1, a Viunalikevirus, Is a Broad-Host-Range, High-Efficiency Generalized Transducer That Infects Environmental and Clinical Isolates of the Enterobacterial Genera Serratia and Kluyvera

Miguel A. Matilla[a] and George P.C. Salmond[a]#

[a]Department of Biochemistry, University of Cambridge, Tennis Court Road, Cambridge, UK, CB2 1QW.

Running title: *Characterization of the Vil-like transducing phage φMAM1*

Keywords: Bacteriophage, Viunalikevirus, *Serratia*, transduction, horizontal gene transfer, oocydin A

Address correspondence to George P.C. Salmond, Department of Biochemistry, University of Cambridge, Tennis Court Road, Cambridge, UK, CB2 1QW. Tel: +44 (0)1223 333650; Fax: +44 (0)1223 766108; E-mail: gpcs2@cam.ac.uk

ABSTRACT

Members of the enterobacterial genus, *Serratia,* are ecologically widespread and some strains are opportunistic human pathogens. Bacteriophage φMAM1 was isolated on *Serratia plymuthica* A153, a biocontrol rhizosphere strain that produces the potently-bioactive antifungal and anticancer haterumalide, oocydin A. The φMAM1 phage is a generalized transducing phage that infects multiple environmental and clinical isolates of *Serratia spp.* and a rhizosphere strain of *Kluyvera cryorescens*. Electron microscopy allowed classification of φMAM1 in the family *Myoviridae*. Bacteriophage φMAM1 is virulent, uses capsular polysaccharides as receptor and can transduce chromosomal markers at frequencies of up to 7 x 10^{-6} transductants per p.f.u. We also demonstrated transduction of the complete 77-kb oocydin A gene cluster and heterogeneric transduction of a Type III Toxin-Antitoxin-encoding plasmid. These results support the notion of the potential ecological importance of transducing phages in the acquisition of genes by horizontal gene transfer. Phylogenetic analyses grouped φMAM1 within the VilI-like bacteriophages and genomic analyses revealed that the major differences between φMAM1 and other VilI-like phages arise in a region encoding the host-recognition determinants. Our results predict that the wider genus of VilI-like phages could be efficient transducing phages - with obvious implications for the ecology of horizontal gene transfer, bacterial functional genomics and synthetic biology.

INTRODUCTION

Bacteriophages (phages) are ubiquitous obligate viral parasites of bacteria that reproduce, in concert with their hosts in diverse natural environments (1,2). Bacteriophage abundance correlates with bacterial population densities in a given niche and the global phage population has been estimated at over 10^{31} phages, reflecting over 10^{25} infections per second (3,4). This intimate interaction between phages and their hosts results in rapid co-evolution that has been observed under both natural environmental and laboratory conditions (5-7).

Since discovery in the early 1900s, phages have been used as therapeutic agents in human infections (8,9), but also as alternative biocontrol agents in agriculture, sewage treatment and in the food industry (10-13). Furthermore, phage display technology has proved useful in cancer studies and for the delivery of vaccines (12,13). Additionally, transducing phages have been important tools in basic bacterial genetics, functional genomics and synthetic biology applications (13-15).

Together with transformation and conjugation, transduction is one of the three main classes of horizontal gene transfer (HGT) in bacteria. In generalized transduction, phages accidentally package large fragments of host bacterial DNA instead of the viral genome. The generated transducing particles adsorb normally and inject DNA into a recipient bacterium. The injected bacterial DNA may integrate by homologous recombination into the genome of the recipient host, resulting in a stable bacterial transductant (14,16). Transducing phages have been used extensively in genetic manipulations, including bacterial strain engineering, transposon mutagenesis and plasmid transfer (14,16).

Bacteria of the genus *Serratia* belong to the family *Enterobacteriaceae*. *Serratia* species are widely distributed, being commonly found in water, soil, plants, animals and man; some species are opportunistic human pathogens (17). Although *Serratia plymuthica* strains have been isolated from diverse environments, they are mostly associated with

plants and are considered to be plant-growth promoting bacteria and excellent biocontrol agents for many fungal and oomycete plant diseases (18). *Serratia plymuthica* A153 was isolated from the rhizosphere of wheat (19) and produces several halogenated macrolides, haterumalides (20). Haterumalides – also known as oocydins - were among the first polyketides found to be synthesised by *Serratia* species (21) and they have been shown to exhibit anti-cancer, antifungal, anti-oomycete and anti-hyperlipidemic properties (20-23). Recently, we isolated and sequenced the new VilI-like *Serratia* phage, ϕMAM1 (24). Here, we analyse the genome and report the morphological and biological characterization of φMAM1, a generalized transducing phage that is able to infect many environmental and clinical isolates from the *Serratia* and *Kluyvera* genera.

MATERIALS AND METHODS

Bacterial strains, plasmids, phages, culture media and growth conditions. Bacterial strains and plasmids used in this study are listed in Tables 1 and A1. *Serratia, Kluyvera* and their derivative strains were routinely grown at 30 ºC, unless otherwise indicated, in Luria Broth (LB; 5 g yeast extract l^{-1},10 g Bacto tryptone l^{-1} and 5 g NaCl l^{-1}), Potato Dextrose (24 g potato dextrose broth l^{-1}) or minimal medium (0.1%, w/v, $(NH_4)_2SO_4$, 0.41 mM $MgSO_4$, 0.2% (w/v) glucose, 40 mM K_2HPO_4, 14.7 mM KH_2PO_4, pH 6.9–7.1). *Escherichia coli* strains were grown at 37 °C in LB. *Escherichia coli* DH5α was used for gene cloning. Media for propagation of *E. coli* β2163 were supplemented with 300 μM 2,6-diaminopimelic acid (DAPA). When appropriate, antibiotics were used at the following final concentrations (in μg ml^{-1}): ampicillin, 100; kanamycin, 25 (*E. coli* strains) and 75 (*Serratia* strains); streptomycin, 50; tetracycline, 10. Sucrose was added to a final concentration of 10% (w/v) when required to select derivatives that had undergone a second cross-over event during marker exchange mutagenesis. Unless indicated, the growth temperature for

S. plymuthica A153, 30 ºC, was used for the phage incubations. Phages were stored at 4 ºC in phage buffer (10 mM Tris-HCl pH 7.4, 10 mM $MgSO_4$, 0.01% w/v gelatine) over a few drops of $NaHCO_3$-saturated chloroform.

φMAM1 phage isolation and phage lysate preparation. Treated sewage effluent was collected from the sewage treatment plant at Milton, Cambridge (United Kingdom) (24). Briefly, a 10 ml sample of the effluent was filter sterilized. Then 500 µL of the sterilized effluent was mixed with 200 µL of a *Serratia plymuthica* A153 overnight culture and 4 mL of top LB-agar (LBA, 0.35% w/v agar) and poured as an overlay onto LBA plates (1.5% w/v agar). Plates were incubated overnight at 30 ºC and single phage plaques were picked with a sterile toothpick into 0.2 ml phage buffer and shaken with 20 µL of chloroform to kill any bacteria. Phages obtained were plaque-purified three times. High-titre phage lysates were then obtained as described Petty *et al.* (25). Phages were titrated by serial dilutions in phage buffer and the phage titre determined in plaque-forming units (p.f.u.) per millilitre.

φMAM1 genome sequencing. Genomic DNA sequencing was performed using 454 DNA pyrosequencing technology as described previously (24). The preparation of the 454 library was done by nebulisation using GS FLX Titanium Rapid Library Preparation Kit following the manufacturer´s instructions (Roche, Cat. No. 05608228001). The shearing was performed with nitrogen gas at a pressure of 30 psi (2.1 bar) for 1 min. The assembly used 257,858 reads or 102.6 MB of raw data to give 650X coverage of the genome.

Genome annotation and bioinformatics. Annotation of φMAM1 genome and identification of tRNAs was performed as described previously (24). Putative bacteriocins were identified using the web-based bacteriocin mining tool BAGEL2 (University of Groningen, The Netherlands). Artemis software (Wellcome Trust Sanger Institute) was used to visualize and annotate the φMAM1 genome. Genome comparison analyses were

performed employing the Artemis Comparison Tool and EMBOSS Stretcher (European Bioinformatics Institute). The genomic organization and annotation of the seven previously reported VilI-like enterobacterial bacteriophages (26) were used to determine the location of ORF1 in φMAM1. The CGView Comparison Tool (27) was employed to visualize the φMAM1 genome and to generate Figure 3. Multiple sequence alignments of phage proteins were performed using ClustalW2 (European Bioinformatics Institute). To analyse and identify motifs in promoter regions, 100 bp sequences upstream of the start codons were extracted using extractUpStreamDNA (http://lfz.corefacility.ca/extractUpStreamDNA/) and analyzed using the MEME Suite (28). Candidate late promoters in φMAM1 were identified by using the T4 late promoters conserved consensus sequence (TATAAATA). Rho-independent transcription terminators were identified by examining the secondary structure of the DNA using ARNold (http://rna.igmors.u-psud.fr/toolbox/arnold/index.php). The phylogenetic analyses were performed with the MEGA software v5.10 (29). The φMAM1 GenBank submission file was generated using Sequin (NCBI). The complete genome sequence of φMAM1 is available in GenBank under Accession Number JX878496.

Electron microscopy

High-titre lysates for transmission electron microscopy were obtained as described by Petty *et al.* (25) using 0.35% (w/v) LB agarose instead of 0.35% (w/v) LB agar overlays. Twenty-five microlitres of high-titre φMAM1 phage lysates (≥ 3 x 10^{10} p.f.u. ml^{-1}) were absorbed onto copper, 400 mesh grids with holey carbon support films (Agar Scientific, Stansted, UK). Copper grids were discharged in a Quorum/Emitech K100X (Quorum, Ringmer, UK) prior to use. After 1 min, excess phage suspension was removed with filter paper and phage samples were negatively stained by placing the grids in 25 µl drops of 2% ammonium tugstate containing 0.1% trehalose (pH 7.0) or 2% aqueous uranyl acetate

(pH 4.0) for 1 min. The grids were then blotted on filter paper to remove the excess solution and allowed to air-dry for 10 minutes. Phages were examined by transmission electron microscopy, in the Multi-Imaging Centre (Department of Physiology, Development and Neuroscience, University of Cambridge) using a FEI Tecnai G2 transmission electron microscope (FEI, Oregon, USA). The accelerating voltage was 120.0 kV and images were captured with an AMT XR60B digital camera running Deben software.

Host range determination

A collection of enterobacterial strains was assembled to test their sensibility to φMAM1. Top agar overlays containing 4 ml of 0.35% (w/v) LBA and 200 µl of an overnight culture of the bacteria strain to test were poured onto a solid LBA plate and allowed to set. A 10 µl sample of serial dilution high-titre phage lysate of φMAM1 was spotted onto each bacteria overlay and the plates were incubated overnight at 30 ºC or 37 ºC. Ten microlitres of phage buffer were also added as negative dilution control. After incubation, each plate was scored for lysis. Efficiency of plaquing (EOP) was determined by dividing the phage titre of the φMAM1-sensitive strain by that of the wild type reference strain, *Serratia plymuthica* A153. EOP assays were performed in triplicate.

Transduction assays

Phage lysates were prepared on bacterial strains carrying the desired mutation or plasmid. Phages were initially tested for their ability to transduce the Tn-KRCPN1 transposon from *oocJ*::Tn-KRCPN1 and *admK*::Tn-KRCPN1 mutations into wild type *S. plymuthica* A153. The transduction protocol was optimized based on the incubation time, temperature, multiplicity of infection (m.o.i.) and number of bacterial cells. An appropriate volume of a high-titre transducing lysate was added to a 10 ml overnight culture of the recipient strain (~1 x 10^{10} total bacterial cells) to give the desired m.o.i. The mixture was incubated at 30 ºC for 30 minutes (1 h for *Sma* 12), pelleted by centrifugation (4.000 g for 10 min at 4 ºC)

and washed twice with 10 ml of LB to remove any remaining lysate. The cells were resuspended in 5 ml of LB and 100 µl aliquots of the cell mixture were spread onto LBA plates containing the appropriate antibiotic and the plates were incubated overnight. When the cell mixture was resuspended in small volumes (e.g. 300 µl of LB) and spread onto LBA plates, we observed a reduction in the transduction efficiency due to phage superinfection that caused lysis of transductant colonies. The transductants obtained were streaked out three times prior to use to reduce or eliminate any bacteriophage carry-over. Transductants were confirmed by screening the antibiotic resistant colonies for coinheritance of a secondary phenotype of either antifungal and antibacterial properties, auxotrophy or cellulose production (see supplementary information). During the transduction assays, controls for spontaneous resistance to antibiotics were determined by spreading 100 µl of the overnight culture onto LBA plates containing the relevant antibiotic. A 100 µl volume of the high-titre lysate was also spread on non-LBA plates to confirm lysate sterility. Transduction efficiency was defined as the number of transductants obtained per p.f.u.

One-step growth curve and burst size

One step growth curve experiments were performed as described previously (25). Briefly, overnight bacterial culture were adjusted to OD_{600} 0.02 in 25 ml LB in a 250 ml flask and grown in a water bath at 30 ºC with orbital shaking (225 r.p.m.). At OD_{600} 0.1, 10 ml of the bacterial culture were removed into a sterile tube and pelleted at 4.000 x g for 10 min at 4 ºC. Once the supernatant was removed, the pellet was resuspended in 10 ml of fresh LB and phage samples were added at an m.o.i. of 0.001. The same amount of phages was also added to 10 ml of LB, as a negative control. Phages were allowed to adsorb for 5 min at room temperature without shaking and the supernatant containing any unadsorbed phages was removed by centrifugation at 4.000 x g for 10 min at 4 ºC. Pellets were

196 resuspended in 10 ml LB, added to 15 ml LB in a 250 ml conical flask and the cultures
197 were grown in a shaking water bath as described previously. Every 10 min, samples were
198 taken and immediately titrated to determine the number of p.f.u. The final growth curve
199 represents the number of phages per initial infectious centre.

200 **Phage adsorption**

201 Phage adsorption experiments were carried out as described previously (25). Briefly, 10 ml
202 overnight cultures of the bacterial host, or non-host bacterial control (*Serratia marcescens*
203 Db11), were infected with φMAM1 at an m.o.i. of 0.01, mixed briefly and placed on a tube
204 roller at 30 ºC. A bacteria-free negative control was created by adding the same amount of
205 phage to 10 ml of LB. One hundred microlitre samples were removed every 5 min and
206 added to 900 µl of phage buffer and 30 µl of chloroform, mixed for 5 seconds and
207 centrifuged at 13.000 x g for 1 min. The number of unadsorbed φMAM1 phage particles
208 was determined by titrating the supernatant on 0.35% (w/v) LBA lawns, as described
209 previously. Phage adsorption to bacteria was expressed as the number of free φMAM1
210 particles per millilitre remaining in the supernatant, and expressed as a percentage of the
211 number of p.f.u. ml^{-1} in the bacteria free negative control.

212 **Transposon mutagenesis and isolation of phage-resistant mutants.**

213 Random transposon mutagenesis of *S. plymuthica* A153 using Tn-KRCPN1 was
214 performed as follows. In a biparental conjugal mating, 500 µl of overnight cultures *of E. coli*
215 β2163 (pKRCPN1) and *S. plymuthica* A153 were mixed, collected by centrifugation,
216 resuspended in 30 µl of fresh LB, and spotted on an LB agar plate supplemented with 300
217 µM DAPA. After overnight incubation at 30 °C, cells were scraped off the plate and
218 resuspended in 1 ml of LB. φMAM1-resistant mutants were selected by mixing 100 µl of
219 the resuspended mating patch with 200 µl phage lysate (≥ 1 x 10^{11} p.f.u. ml-1) and 4 ml of
220 0.35% (w/v) LBA containing 75 µg ml^{-1} kanamycin. The mixture was poured onto a solid

LBA plate, allowed to set and incubated overnight at 30 ºC. DAPA was not added to LBA medium to allow counterselection of the *E. coli* donor. The insertion site of transposon Tn-KRCPN1 in the φMAM1-resistant mutants was determined using random primed PCR following the method described previously (30).

Supplementary experimental procedures. *In vitro* nucleic acid techniques, construction of the A153 OocKmSm strain, phenotypic analysis of transductans and toxin-antitoxin abortive infection assays are given as supplementary information.

RESULTS

Isolation of φMAM1

During environmental screening for new bacteriophages infecting clinical and environmental isolates of *Serratia*, we isolated 17 new phages infecting the haterumalide-producing strain, *Serratia plymuthica* A153 (24). Isolated, plaque purified phage lysates of high titre were screened for their ability to transduce Tn-KRCPN1 chromosomal mutations into the A153 wild type strain. Of the 17 new phages, φMAM1 was the only transducing phage and was selected for further characterization.

φMAM1 forms plaques ranging between 6.6 ± 0.9 and 1.2 ± 0.3 mm in diameter when the phages were titrated and plated in 0.2-0.8% agar overlays (Fig. A1). Within the tested temperatures, ranging between 25 and 37 ºC, no differences in plaque formation were observed (data not shown). φMAM1 viability was unaffected by the addition of chloroform during storage in phage buffer at 4 ºC and phage lysates retained high viability during the period of this study, 2 years (>65% of the initial titre).

φMAM1 morphology

Using transmission electron microscopy, the morphology of φMAM1 was determined. φMAM1 has an icosahedral and isometric head measuring 90 ± 2 nm from flat face to flat

face. Its contractile tail measures 120 ± 2 nm long and 21 ± 2 nm in diameter when extended, or 57 ± 2 nm long and 26 ± 2 nm in diameter when contracted (Fig. 1). The φMAM1 tail consists of a 11 ± 1 nm neck with a collar, a tail tube surrounded by a contractile sheath showing 24 transverse striations, a baseplate and a complex system of tail spikes (Fig. 1). Based on its morphology and according to Ackermann´s (31) classification, φMAM1 was grouped into the order *Caudovirales* within the *Myoviridae* family, which comprises 25% of the tailed bacteriophages and includes the *Escherichia coli* phage, T4. Morphologically, φMAM1 is very similar to *Salmonella* phages Vi01 (32), φSH19 (33) and SFP10 (34), *Shigella* phage φSboM-AG3 (35), *E. coli* phages CBA120 (36) and PhaxI (37) and *Dickeya* phage LIMEstone1 (11). All these ViI-like enterobacterial bacteriophages have been described recently as members of a newly proposed genus within the *Myoviridae* family, "Viunalikevirus" (26). The adsorption "organelle" in "Viunalikevirus" members shows two conformations consisting of "prongs" and "umbrella-like" filaments with rounded tips, both associated with the baseplate (26). Both conformations were observed in φMAM1 (Fig. 1A,B) and each of the "umbrella-like" structures shows 4 short filaments attached to the baseplate by a stalk (Fig. 1B).

Biological characterization of φMAM1

We evaluated the ability of φMAM1 to lyse host bacteria in liquid cultures by adding phages at different m.o.i. to *S. plymuthica* A153 cultures. φMAM1 infection caused a reduction in growth rate followed by a cessation of bacterial growth 30 and 90 min after phage addition, respectively. Bacterial lysis caused a decrease in the turbidity of the culture two hours after phage addition (Fig. 2A). However, a resumption of growth was observed in A153 after a prolonged incubation period (data not shown). This resumption was associated with the emergence of phage resistant mutants, since A153 isolates from late infected cultures showed φMAM1 resistance in agar lawn assays.

Phage adsorption assays confirmed that φMAM1 adsorbs rapidly to *S. plymuthica* A153, with more than 95% of the phage particles adsorbed within the first 5 min. The number of adsorbed phage particles reached an apparent maximum 30 min post-mixing (Fig. 2B) and this time was chosen as the incubation time in the A153 transduction assays (see below).

To determine the burst size of φMAM1, one-step growth curves were carried out. φMAM1 showed a latent period of ~20 min and a rise period, where the phage particles were released, of around 40 min. The average burst size was more than 300 phage particles per initial infection centre (Fig. 2C).

Host range of the virulent bacteriophage φMAM1

Sensitivity to φMAM1 of a collection of 25 environmental and clinical isolates of *Serratia marcescens* (*Sma*) (38) and 30 enterobacterial strains isolated from the rhizosphere of agronomic crops (39) was investigated by spotting phage lysates onto bacterial lawns. Bacterial clearing was observed on agar lawns of 17 *Sma* strains and in the rhizobacterium, *Kluyvera cryorescens* 2Kr27 (Table 1; Fig. A1). The plaques formed in the sensitive strains varied in size and were clear in most strains, but turbid in *Sma* 0006, *Sma* 1047, *Sma* 3127, *Sma* 3078V and *Sma* S6. However, subsequent phage titrations showed no obvious plaque formation in *Sma* 1695 and *Sma* 2595. We showed that the observed lysis in the latter two strains was not due to a bacteriocin present in the phage lysate (data not shown). Further adsorption assays confirmed that φMAM1 adsorbs to *Sma* 1695 and *Sma* 2595, but with low efficiencies (Fig. A2). For strains where φMAM1 was able to form plaques, the efficiency of plaquing (EOP) was similar, except on *Sma* 365 (EOP of 6.1 x 10^{-3}), suggesting that there was no host controlled restriction system active against this phage in most strains (Table 1).

As φMAM1 formed turbid plaques in several strains we used the protocol described by Petty *et al*., (25), to test for lysogeny in *Sma* 0006, *Sma* 1047, *Sma* 3127, *Sma* 3078V and

297 *Sma* S6 after φMAM1 exposure. The results were universally negative and it is reasonable
298 to assume that this is either a virulent phage or a temperate phage with a low frequency of
299 lysogeny.
300 Other enterobacterial strains belonging to *Dickeya, Escherichia, Pectobacterium,*
301 *Citrobacter, Photorhabdus, Yersinia, Salmonella*, *Pantoea* and *Enterobacter* genera were
302 also tested for susceptibility to φMAM1 infection. None of the strains tested showed signs
303 of φMAM1 sensitivity.
304
305 **φMAM1 is a generalized transducing phage**
306 As described above, φMAM1 was the only A153 infecting phage able to transduce
307 mutations between A153 strains. No differences in the transduction efficiency were
308 observed at different temperatures (e.g. 25, 30 and 37 ºC; not shown) or using different
309 number of cells (e.g. 10^8, 10^9 and 10^{10} total bacterial cells) (Table 2). Transduction
310 efficiency was higher at an m.o.i of 0.01 and 0.1 (>10^{-6} transductants obtained per p.f.u).
311 However, the transduction efficiency decreased with higher m.o.i. probably due to φMAM1
312 superinfection killing of the transductants (Table 2). In fact, during the transduction assays,
313 the size of the transductants colonies after overnight incubation decreased as the m.o.i.
314 values increased and some phage "nibbling" was observed at the edges of these colonies.
315 Transduction efficiencies were determined in A153 and *Sma* 12 for several chromosomal
316 markers including mutations in the oocydin A biosynthetic genes *oocJ* and *oocU,* the
317 antibiotic biosynthetic genes *admH* and *admK* and the cellulose synthase regulator
318 encoding gene *bcsB*, among others. Transduction efficiencies between 1.1 x 10^{-6} and 4.2 x
319 10^{-6} were observed for the different chromosomal markers in the wild type reference strain
320 A153 (Table 3). The frequency ranged from 2.3 x 10^{-6} to 7.2 x 10^{-6} in *Sma* 12 (Table 3).
321 Transduction of a kanamycin derivative version of pECA1039 from *S. plymuthica* A153 to
322 *Sma* 12 and *Kluyvera cryorescens* 2Kr27 was also demonstrated. The plasmid pECA1039,

isolated from the Gram-negative bacterium *Pectobacterium atrosepticum* (40), encodes the first known Type III Toxin-Antitoxin (TA) system, ToxIN, bifunctional as an abortive infection system active against many phages. However φMAM1 was not aborted by the ToxIN system. Although the plasmid transduction efficiencies were relatively high, these were one order of magnitude lower than those obtained for the transduction of chromosomal markers (Table 3).

φMAM1 genome analysis

φMAM1 has a dsDNA of 157,834 bp (98.5 x 10^6 Da) encoding 198 putative ORFs and three tRNAs genes, tRNA-Pro (CCU), tRNA-Met (AUG) and tRNA-Cys (UGU) (Fig. 3; Table A2) (24). Three different start codons, ATG (94.0%), GTG (3.5%) and TTG (2.5%), were identified. The coding sequences of φMAM1 represent 91.6% of the genome with a GC content of 52.5%. Based on BLASTP similarities and the presence of conserved domains, a predicted function was assigned to 39.8% of the identified ORFs. Within the 60.2% of the genes encoding hypothetical proteins, 27.3% of them were unique to φMAM1. Genome comparison analyses showed that the genome of φMAM1 is between 52.7 and 54.2% identical at the DNA level to the genomes of the seven sequenced VilI-like phages and shares between 59.0 and 64.6% of their putative ORFs (Fig. 3-4; Table A2 and A3).

The highly homology observed between φMAM1 and VilI-like phages led us to investigate their phylogenetic relationships. Thus, the amino acid sequences of a structural protein (major capsid protein) and a non-structural protein (DNA polymerase) were chosen to perform phylogenetic analyses. Previously, major capsid proteins and DNA polymerase were often used as phylogenetic markers (26,34,41). As expected from the phage morphology and the genomic comparison analyses, the phylogeny revealed that φMAM1 is closely related to VilI-like phages (Fig. A3).

349

350 ***Transcription, regulatory sequences and translation***

351 The analysis of the promoter regions of the φMAM1 genes allowed us to identify the motif
352 TTCAATAA[N_{12}]TATtAT in the promoters of 27 φMAM1 genes (Fig. A4A). Most (81.4%) of
353 the φMAM1 genes containing this upstream consensus sequence encode hypothetical
354 proteins making it difficult to predict in which stage of the lytic cycle they may be
355 expressed. However, the motif shows similarity with the consensus sequence of the *E. coli*
356 RpoD-dependent promoters (TTGACA[N_{15-18}]TATAAT) (42) and to the conserved motif
357 identified in T4 early promoters (43) perhaps indicating that these genes are expressed in
358 early stages of the phage lytic cycle.

359 In general, late transcription is responsible for the synthesis of phage structural
360 components, besides other recombination and replication factors (43). Based on the
361 consensus sequence of T4 late promoters (TATAAATA) (44), we identified 16 putative late
362 promoters (Fig. A4B). Seven of them, including P_{MAM_038} (upstream of a tail spike head-
363 binding protein gene), P_{MAM_135} (baseplate hub subunit), P_{MAM_142} (Gp32 ssDNA binding
364 protein) and P_{MAM_143} (Gp19 baseplate tail tube) are expected to be late genes. Several
365 proteins have been described as involved in late transcription in T4-related phages and
366 φMAM1 encodes orthologs of all of them - including the transcription co-activator Gp33
367 (MAM_140), sigma factor Gp55 (MAM_108), sliding clamp protein Gp45 (MAM_078) and
368 the clamp-loader proteins Gp44 (MAM_079) and Gp62 (MAM_080) (43,44). Thirty six Rho-
369 independent terminators were identified in the genome of φMAM1, four of them predicted
370 to be on late transcripts (Fig. A4C).

371

372 ***Structural components***

373 Mass spectrometry analysis identified 41 structural proteins in Vi01 (32) and 39 in
374 LIMEstone1 (11), two VilI-like phages. However, the function of 33% (11) and 41% (32),

respectively, of the identified structural proteins is unknown. With the exception of 6 and 4 unknown structural proteins identified in Vi01 and LIMEstone1, respectively, orthologs for the remaining structural proteins were found in φMAM1 (Table A2). However, genome comparison analyses showed that major differences were observed in a 14.7-kb region encoding the host-recognition elements, the tail spike proteins (TSPs) (Fig. 3-4; Table A2). Other φMAM1 structural proteins are described in the supplementary material.

Most of the sequenced ViI-like phages encode four tail spike proteins (26) and the presence of these TSPs has been confirmed by mass spectrometry analyses in Vi01 (32) and LIMEstone1 (11). φMAM1 also encodes four putative TSPs, three of which (MAM_031, MAM_034, MAM_037) contain a pectate lyase domain (Table A2). The TSP MAM_031 is a 987 amino acid protein and BlastP analyses showed that its first 262 amino acids are 45-49% identical (64% similar) to the N-terminal region of TSPs encoded by all the seven sequenced ViI-like phages. However, the N-terminal regions of the other three putative TSPs (MAM_034, MAM_037, MAM_038) are less conserved and appear to be more specific to φMAM1. Thus, MAM_034 is 37-39% identical (53-55% similar) from amino acid 23 to amino acid 114 to TSPs present in SFP10, CBA120 and PhaxI, whereas the amino acids 25-211 of the N-terminal region of MAM_037 are 34% identical (54% similar) to the TSP-1 of φSH19. Finally, the first 97 residues of the 602 amino acid TSP MAM_038 are 29% identical (46% similar) to the TSP Vi01_170c of the *Salmonella* phage Vi01 (Table A2). Interestingly, the BlastP analyses also showed that the C-terminal regions of the four φMAM1 putative TSPs show similarity to several proteins of unknown function encoded by *Serratia plymuthica* AS9 (45), *Serratia plymuthica* AS12 (46) and *S. proteomaculas* 568 (47), bacterial strains closely related to the φMAM1 host, *S. plymuthica* A153.

Capsular antigen is the receptor for φMAM1

Group 1 capsular polysaccharides (CPS) and lipopolysaccharide (LPS) O-antigen biosynthetic gene clusters of *Enterobacteriaceae* have important common features. In fact, research on the biosynthesis of LPS O-antigens has been extrapolated to understand the assembly of CPS (48). Thus, both CPS and LPS O-antigen gene clusters share many genes and they are located between the *galF* and *gnd* genes in strains belonging to *Escherichia*, *Salmonella*, *Shigella* and *Enterobacter* genera (49-52). However, it is the presence of the *wza, wzb* and *wzc* genes that differentiates these CPS and LPS loci (48).

All the A153 phage resistance mutations mapped in a 17.6-kb region between *galF* and *gnd* (Fig. A5). The 17.6-kb region consists of 13 genes predicted to form an operon (Fig. A5) and, consequently, the insertion of the Tn-KRCPN1 transposon may cause polar effects in the expression of the downstream genes. In this region, *wza*, *wzb* and *wzc* genes are involved in the synthesis, export and regulation of CPS (48,53). The hexose-1-phosphate transferase encoding gene (*wbaP*) was proposed to be involved in the initiation of the capsular polysaccharide synthesis (48). The polysaccharide can be extended by the action of glycosyltransferases, four of which are encoded by genes in this region. The region also contains the gene *wzx*, encoding a flippase required for the translocation of the CPS biosynthetic units across the inner plasma membrane (53). Not surprisingly, the region also encodes a hypothetical protein that is 31% identical (49% similar) to the C-terminal region of the TSP MAM_034 protein.

During the characterization of the phage resistant mutants, we noted that they exhibited a "rough" colony morphology characteristic of some CPS defective mutants and they showed the same antifungal activity as the parental A153 strain (Fig. A5). Adsorption of φMAM1 to all the phage-resistant mutants was abolished, confirming the role of CPS as receptors (Fig. 2B).

Mobilization of the oocydin A gene cluster by transduction

427 The abundance and diversity of secondary metabolite gene clusters in some bacterial
428 strains, and their irregular distribution, raised the possibility of horizontal transfer of such
429 gene clusters between bacterial strains (54). Recently, we identified a 77-kb gene cluster
430 involved in the biosynthesis of the haterumalide, oocydin A (*ooc*) (30). Given the high
431 transduction efficiency and its large genome size, we decided to use φMAM1 as a genetic
432 tool for mobilizing the *ooc* gene cluster. Thus, we constructed the strain *S. plymuthica*
433 A153 OocKmSm containing a kanamycin resistance and a streptomycin resistance
434 cassette up- and downstream of the *ooc* gene cluster, respectively. The OocKmSm strain
435 was the donor strain used to transduce the *ooc* gene cluster into the non-oocydin A
436 producing strain OocEV, containing in-frame deletions in *oocE* and *oocV*. Among the
437 transductants, 17.7 % and 9.5 % of the streptomycin and kanamycin resistant colonies
438 showed restoration of the oocydin A production, respectively (Table 4; Fig. 5). The *ooc*
439 gene cluster was transduced into OocEV with a frequency of 1.9×10^{-7} and the production
440 of the haterumalide was fully restored in the kanamycin and streptomycin doubly resistant
441 colonies (Table 4). We also tried to transduce the *ooc* gene cluster into the other φMAM1
442 sensitive strains. However, no transductants were obtained with these strains presumably
443 due to insufficient DNA homology between the donor (A153) and the recipient strains to
444 enable homologous recombination.

445 **DISCUSSION**

446 Horizontal gene transfer (HGT) is a powerful source of genomic diversity and contributes
447 actively to the rapid evolution of prokaryotes (55). In fact, it has been estimated that up to
448 80% of known bacterial and archaeal genomes may be affected by HGT (56). From an
449 ecological perspective, the acquired genes may represent an adaptive advantage for the
450 microorganisms under certain environmental conditions (57,58). Transduction has been
451 described in natural environments such as sewage, fresh and sea water and on plant

leaves reflecting its importance in microbial ecology and in the evolution of microbial populations (14,56).

Several *Serratia* transducing bacteriophages have been identified previously (25,59,60). However, to our knowledge, φMAM1 is the first transducing phage described for *Serratia plymuthica*. Compared with other enterobacterial phages (25,61,62), the high transduction efficiency mediated by φMAM1, together with its large genome (it can transduce around 3% of the A153 host genome) and its wide host range, makes this new phage an extraordinary tool for bacterial genetics. Additionally, given the DNA homology between φMAM1 and the other sequenced ViI-like phages (Table A3; Fig. 3-4), it remains possible that all these "Viunalikevirus" bacteriophages will be highly efficient transducers. Consistent with this notion, *Salmonella* phage Vi01 was shown to be a transducing phage twenty years ago (63).

We have shown recently that the oocydin A gene cluster is present in four plant associated bacteria belonging to *Serratia* and *Dickeya* genera (30). The fact that the genomic context of the *ooc* gene cluster in three of these bacteria is different, together with the identification of sequences similar to a bacteriophage P4 integrase bordering the cluster in one of the strains, suggests that the gene cluster was previously acquired by HGT (30). High bacterial density has been associated with elevated transduction rates (64), perhaps indicating that the rhizosphere may be a niche conducive to higher transduction frequencies. In agreement with this idea, we have found that several *Serratia* strains isolated from the rhizosphere of the same crop are able to produce oocydin A (M.A. Matilla and G.P.C. Salmond, unpublished data). This observation indicates that the *ooc* gene cluster is more widespread than perhaps expected and it is possible that it has been transferred between rhizosphere strains by transduction.

φMAM1 contains three tRNA genes located together in a cluster. Although tRNA-Met is conserved within most the sequenced ViI-like phages, thus far tRNA-Pro and tRNA-Cys

genes are unique to φMAM1. The function of phage tRNA is still an open debate but it has been suggested that a positive correlation exists between the tRNA distribution and phage codon usage (65). Although this correlation is absent in φMAM1 (data not shown), phage tRNAs have been associated with overcoming differences in the GC content between the phages and their hosts (66). Interestingly, the G+C content of the φMAM1 tRNA genes (56.2%) and the genome of its host *S. plymuthica* A153 (55.9%) (24) are similar.

Many reports have reported promiscuity in enterobacterial phages (34,35,60,67,68) and φMAM1 is another noteworthy example. φMAM1 infects 68% of the *Serratia marcescens* strains tested and a rhizobacterial strain from the *Kluyvera* genus. φMAM1 sensitive strains include 7 environmental and 10 clinical isolates, including the model bacterium *Sma* 365 and the carbapenem-resistant, *Sma* S6. Additionally, the C-terminal region of the TSPs from φMAM1 show similarity to several hypothetical proteins encoded by strains such as *Serratia proteamaculans* (*Spro*) 568, a rhizobacterial strain with a genome highly similar to that of A153 (47). TSP proteins are involved in the recognition of host receptor(s) and the analysis of their C-terminal regions has been predicted as a rational approach for the identification of new phage hosts (26,69,70). Strain *Spro* 568 shows interesting biocontrol properties including plant growth promotion and production of exoenzymes (47), however its genome does not contain genetic information for the synthesis of oocydin A. We were able to transduce the complete, functional *ooc* gene cluster back into the non-oocydin A producer strain OocEV at high efficiency (Table 4, Fig. 5). Thus, φMAM1 might prove an effective tool for mobilizing the *ooc* gene cluster into non-oocydin producers, thereby engineering synthetic derivative strains with enhanced biocontrol properties, perhaps mimicking a process that is likely to be occurring naturally in the environment.

Mechanisms of bacterial defence against bacteriophages include the mutation of host receptors, restriction of the incoming phage DNA, abortive infection (i.e. through toxin-antitoxin systems) and CRISPR-Cas systems (71). Toxin-antitoxin (TA) systems are

504 generally comprised of two genes encoding a toxin component and its cognate antitoxin
505 (72). TA loci are widespread in bacteria and they have been found in plasmids and
506 bacterial chromosomes, strongly implicating HGT in the dissemination of these systems
507 (72,73). In 2009, we identified and characterised the first Type III protein-RNA TA system,
508 encoded by the plasmid pECA1039 of the phytopathogen, *Pectobacterium atrosepticum*
509 (40). Using φMAM1, transduction of pECA1039-km3 between different species of *Serratia*
510 and between two bacterial genera was demonstrated (Table 3). Given the importance of
511 anti-viral abortive infection systems in the population biology of bacteria that are constantly
512 assaulted by viral parasites, these observations reinforce the notion that phages are key
513 players in the dissemination of important genetic information - and therefore in adaptive
514 bacterial evolution in changing ecological niches. Interestingly, neither the *P. atrosepticum*
515 TA system nor the Type III TA system encoded by the insect pathogenic bacterium
516 *Photorhabdus luminescens* (72) were able to protect *S. plymuthica* A153 from φMAM1
517 infection (not shown) suggesting that this phage evolved the capacity to naturally
518 circumvent the abortive infection system. However, another phage defensive
519 mechanism(s) may be present in the φMAM1 sensitive strains *Sma* 1695 and *Sma* 2595
520 since no plaque formation was observed in these two strains.
521 The recognition of host receptors by VilI-like phages is dependent on tail spikes proteins
522 (TSP) instead of T4-like tail fibers (26). Based on the crystal structure of the C-terminal
523 TSP of the *Salmonella* phage Det7 (69), a phage morphologically similar to φMAM1,
524 several authors have proposed a role for the TSP regions. Thus, the N-terminal region
525 may bind to the phage base plate transferring the signal to the tail structure after phage
526 adsorption whereas the C-terminal region is responsible of the recognition of the host
527 receptor (26,36,69). As observed in other VilI-like phages (26), the C-terminal region of the
528 TSPs from φMAM1 contains domains with enzymatic activity. These enzymatic domains
529 are required for phage infection and it has been proposed that they serve to separate the

phage from cell debris after bacterial lysis (69). TSPs from the ViI-like *Salmonella* phages Vi01 (32) and Det7 (69) contain an acetyl transferase and an O-antigen binding domain, respectively, responsible for the recognition of the exopolysaccharide capsule and LPS as receptors. TSP-2 of the phage φSH19 contains a pectate lyase domain and it was suggested that it may have a role in the cleavage of glycosidic bonds (33). In agreement with these observations, capsular antigen appears to be the receptor for φMAM1 and, interestingly, three of its four TSPs contain a putative pectate lyase domain. Recently, capsular polysaccharides also have been proposed to be the receptor in the ViI-like *Klebsiella* phage o507-KN2-1 (74). Future synthetic biology approaches will involve engineering of highly efficient transducing phages with promiscuous host ranges through exploitation of structural knowledge that underpins the exquisite molecular specificity seen in these phage-host interactions.

ACKNOWLEDGMENTS

This research was supported by the EU Marie-Curie Intra-European Fellowship for Career Development (FP7-PEOPLE-2011-IEF) grant number 298003. The Salmond lab is supported by funding through the Biotechnology and Biological Sciences Research Council (BBSRC, UK). We thank Hazel Aucken and Kornelia Smalla for kindly supplying the environmental and clinical isolates. We would also like to thank Jeremy N. Skepper (Department of Anatomy, University of Cambridge) for assistance in transmission electron microscopy and Alison Rawlinson for technical support.

REFERENCES

1. **Orlova EV.** 2012. Bacteriophages and their structural organisation, p 3-30. *In* Kurtboke I (ed), Bacteriophages. InTechOpen.

555 2. **Koskella B, Meaden S.** 2013. Understanding bacteriophage specificity in natural
556 microbial communities. Viruses **5**:806-823
557 3. **Hendrix RW.** 2003. Bacteriophage genomics. Curr. Opin. Microbiol. **6**:506-511.
558 4. **Lima-Mendez G, Toussaint A, Leplae R.** 2007. Analysis of the phage sequence
559 space: the benefit of structured information. Virology **365**:241-249.
560 5. **Brockhurst MA, Morgan AD, Fenton A, Buckling A.** 2007. Experimental coevolution
561 with bacteria and phage. The *Pseudomonas fluorescens*--Phi2 model system. Infect
562 Genet. Evol. **7**:547-552.
563 6. **Gómez P, Buckling A.** 2011. Bacteria-phage antagonistic coevolution in soil. Science
564 **332**:106-109.
565 7. **Westra ER, Swarts DC, Staals RH, Jore MM, Brouns SJ, van der Oost J.** 2012.
566 The CRISPRs, they are A-Changin': how prokaryotes generate adaptive immunity. Annu.
567 Rev. Genet. **46**:311-339.
568 8. **Abedon ST, Kuhl SJ, Blasdel BG, Kutter EM.** 2011. Phage treatment of human
569 infections. Bacteriophage **1**:66-85.
570 9. **Chhibber S, Kumari S.** 2012. Application of Therapeutic Phages in Medicine, p 139-
571 158. *In* Kurtboke I (ed), Bacteriophages. InTechOpen.
572 10. **Goodridge LD, Bisha B.** 2011. Phage-based biocontrol strategies to reduce
573 foodborne pathogens in foods. Bacteriophage **1**:130-137.
574 11. **Adriaenssens EM, Van Vaerenbergh J, Vandenheuvel D, Dunon V, Ceyssens PJ,**
575 **De Proft M, Kropinski AM, Noben JP, Maes M, Lavigne R.** 2012. T4-related
576 bacteriophage LIMEstone isolates for the control of soft rot on potato caused by 'Dickeya
577 solani'. PLoS One **7**:e33227
578 12. **Haq IU, Chaudhry WN, Akhtar MN, Andleeb S, Qadri I.** 2012. Bacteriophages and
579 their implications on future biotechnology: a review. Virol. J. **9**:9.

580 13. **Henry M, Debarbieux L.** 2012. Tools from viruses: bacteriophage successes and
581 beyond. Virology **434**:151-161.
582 14. **Fineran PC, Petty NK, Salmond GPC.** 2009. Transduction: Host DNA Transfer by
583 Bacteriophages, p 666-679. *In* Schaechter M (ed), The Encyclopedia of Microbiology, 3rd
584 ed. Elsevier, Oxford.
585 15. **Citorik RJ, Mimee M, Lu TK.** 2014. Bacteriophage-based synthetic biology for the
586 study of infectious diseases. Curr Opin Microbiol **19C**:59-69.
587 16. **Masters M.** 1996. Generalized transduction, p 2421-2441. *In* Neidhardt FC, Curtiss III
588 R, Ingraham JL, Lin ECC, Low KB, Magasanik B, Reznikopp WS, Riley M, Schaechter M,
589 Umbarger HE (ed), *Escherichia coli* and *Salmonella typhimurium*: Cellular & Molecular
590 Biology, 2nd ed. ASM Press, Washington, DC.
591 17. **Grimont F, Grimont PAD.** 2006. The Genus *Serratia*, p 219-244. *In* Dworkin M,
592 Falkow S, Rosenberg E, Schleifer KH, Stackebrandt E (ed), The Prokaryotes, vol 6.
593 Springer, New York, NY.
594 18. **De Vleesschauwer D, Hofte M.** 2007. Using *Serratia plymuthica* to control fungal
595 pathogens of plants. CAB Reviews: Perspectives in Agriculture, Veterinary Science,
596 Nutrition and Natural resources **2**:1-12.
597 19. **Hökeberg M, Gerhardson B, Johnsson L.** 1997. Biological control of cereal seed-
598 borne diseases by seed bacterization with greenhouse-selected bacteria. Eur. J. Plant
599 Pathol. **103**:25-33.
600 20. **Levenfors JJ, Hedman R, Thaning C, Gerhardson B, Welch CJ.** 2004. Broad-
601 spectrum antifungal metabolites produced by the soil bacterium *Serratia plymuthica* A153.
602 Soil. Biol. Biochem. **36**:677-685.
603 21. **Strobel G, Li JY, SugawaraF, Koshino H, Harper J, Hess WM.** 1999. Oocydin A, a
604 chlorinated macrocyclic lactone with potent antioomycete activity from *Serratia*
605 *marcescens*. Microbiology **145**:3557-3564.

606 22. **Sato B, Nakajima H, Fujita T, Takase S, Yoshimura S, Kinoshita T, Terano H.**
607 2005. FR177391, a new anti-hyperlipidemic agent from *Serratia*. I. Taxonomy,
608 fermentation, isolation, physico-chemical properties, structure elucidation, and biological
609 activities. J. Antibiot. **58**:634-639.
610 23. **Teruya T, Suenaga K, Maruyama S, Kurotaki M, Kigoshi H.** 2005. Biselides A–E.
611 Novel polyketides from the Okinawan ascidian *Didemnidae* sp. Tetrahedron **61**:6561–
612 6567.
613 24. **Matilla MA, Salmond GP.** 2012. Complete genome sequence of *Serratia plymuthica*
614 bacteriophage φMAM1. J. Virol. **86**:13872-13873.
615 25. **Petty NK, Foulds IJ, Pradel E, Ewbank JJ, Salmond GP.** 2006. A generalized
616 transducing phage (ϕIF3) for the genomically sequenced *Serratia marcescens* strain Db11:
617 a tool for functional genomics of an opportunistic human pathogen. Microbiology
618 **152**:1701-1708.
619 26. **Adriaenssens EM, Ackermann HW, Anany H, Blasdel B, Connerton IF, Goulding**
620 **D, Griffiths MW, Hooton SP, Kutter EM, Kropinski AM, Lee JH, Maes M, Pickard D,**
621 **Ryu S, Sepehrizadeh Z, Shahrbabak SS, Toribio AL, Lavigne R.** 2012. A suggested
622 new bacteriophage genus: "Viunalikevirus". Arch. Virol. **157**:2035-2046.
623 27. **Grant JR, Arantes AS, Stothard P.** 2012. Comparing thousands of circular genomes
624 using the CGView Comparison Tool. BMC Genomics **13**:202.
625 28. **Bailey TL, Boden M, Buske FA, Frith M, Grant CE, Clementi L, Ren J, Li WW,**
626 **Noble WS.** 2009. MEME SUITE: tools for motif discovery and searching. Nucleic Acids
627 Research **37**:W202-W208.
628 29. **Tamura K, Peterson D, Peterson N, Stecher G, Nei M, Kumar S.** 2011. MEGA5:
629 molecular evolutionary genetics analysis using maximum likelihood, evolutionary distance,
630 and maximum parsimony methods. Mol. Biol. Evol. **28**:2731-2739.

631 30. **Matilla MA, Stöckmann H, Leeper FJ, Salmond GP.** 2012. Bacterial biosynthetic
632 gene clusters encoding the anti-cancer haterumalide class of molecules: biogenesis of the
633 broad spectrum antifungal and anti-oomycete compound, oocydin A. J. Biol. Chem.
634 **287**:39125-39138.
635 31. **Ackermann HW.** 2006. Classification of bacteriophages. In *The Bacteriophages*.
636 Calendar, R. (Ed.). New York, USA, Oxford University Press, pp. 8-16.
637 32. **Pickard D, Toribio AL, Petty NK, van Tonder A, Yu L, Goulding D, Barrell B,**
638 **Rance R, Harris D, Wetter M, Wain J, Choudhary J, Thomson N, Dougan G.** 2010. A
639 conserved acetyl esterase domain targets diverse bacteriophages to the Vi capsular
640 receptor of *Salmonella enterica* serovar Typhi. J. Bacteriol. **192**:5746–5754.
641 33. **Hooton SP, Timms AR, Rowsell J, Wilson R, Connerton IF.** 2011. *Salmonella*
642 Typhimurium-specific bacteriophage PhiSH19 and the origins of species specificity in the
643 Vi01-like phage family. Virol. J. **8**:498.
644 34. **Park M, Lee JH, Shin H, Kim M, Choi J, Kang DH, Heu S, Ryu S.** 2012.
645 Characterization and comparative genomic analysis of a novel bacteriophage, SFP10,
646 simultaneously inhibiting both *Salmonella enterica* and *Escherichia coli* O157:H7. Appl.
647 Environ. Microbiol. **78**:58-69.
648 35. **Anany H, Lingohr E, Villegas A, Ackermann HW, She YM, Griffiths M, Kropinski**
649 **A.** 2011. A *Shigella boydii* bacteriophage which resembles *Salmonella* phage ViI. Virol. J.
650 **8**:242.
651 36. **Kutter EM, Skutt-Kakaria K, Blasdel B, El-Shibiny A, Castano A, Bryan D,**
652 **Kropinski AM, Villegas A, Ackermann HW, Toribio AL, Pickard D, Anany H, Callaway**
653 **T, Brabban AD.** 2011. Characterization of a ViI-like phage specific to *Escherichia coli*
654 O157:H7. Virol. J. **8**:430.
655 37. **Shahrbabak SS, Khodabandehlou Z, Shahverdi AR, Skurnik M, Ackermann HW,**
656 **Varjosalo M, Yazdi MT, Sepehrizadeh Z.** 2013. Isolation, characterization and complete

genome sequence of PhaxI: a phage of *Escherichia coli* O157:H7. Microbiology **159**:1629-1638.

38. **Aucken HM, Pitt TL.** 1998. Antibiotic resistance and putative virulence factors of *Serratia marcescens* with respect to O and K serotypes. J. Med. Microbiol. **47**:1105-1113.

39. **Berg G, Roskot N, Steidle A, Eberl L, Zock A, Smalla K.** 2002. Plant-dependent genotypic and phenotypic diversity of antagonistic rhizobacteria isolated from different *Verticillium* host plants. Appl. Environ. Microbiol. **68**:3328-3338.

40. **Fineran PC, Blower TR, Foulds IJ, Humphreys DP, Lilley KS, Salmond GP.** 2009. The phage abortive infection system, ToxIN, functions as a protein-RNA toxin-antitoxin pair. Proc. Natl. Acad. Sci. U.S.A. **106**:894-899.

41. **Yamada T, Satoh S, Ishikawa H, Fujiwara A, Kawasaki T, Fujie M, Ogata H.** 2010. A jumbo phage infecting the phytopathogen *Ralstonia solanacearum* defines a new lineage of the *Myoviridae* family. Virology **398**:135-47.

42. **Harley CB, Reynolds RP.** 1987. Analysis of *Escherichia coli* promoter sequences. Nucleic Acids Res. **15**:2343-2361.

43. **Miller ES, Kutter E, Mosig G, Arisaka F, Kunisawa T, Rüger W.** 2003. Bacteriophage T4 genome. Microbiol. Mol. Biol. Rev. **67**:86-156.

44. **Geiduschek EP, Kassavetis GA.** 2010. Transcription of the T4 late genes. Virol. J. **7**:288.

45. **Neupane S, Högberg N, Alström S, Lucas S, Han J, Lapidus A, Cheng JF, Bruce D, Goodwin L, Pitluck S, Peters L, Ovchinnikova G, Lu M, Han C, Detter JC, Tapia R, Fiebig A, Land M, Hauser L, Kyrpides NC, Ivanova N, Pagani I, Klenk HP, Woyke T, Finlay RD.** 2012. Complete genome sequence of the rapeseed plant-growth promoting *Serratia plymuthica* strain AS9. Stand Genomic Sci. **6**:54-62.

46. **Neupane S, Finlay RD, Alström S, Goodwin L, Kyrpides NC, Lucas S, Lapidus A, Bruce D, Pitluck S, Peters L, Ovchinnikova G, Chertkov O, Han J, Han C, Tapia R,**

683 **Detter JC, Land M, Hauser L, Cheng JF, Ivanova N, Pagani I, Klenk HP, Woyke T,**
684 **Högberg N.** 2012. Complete genome sequence of *Serratia plymuthica* strain AS12. Stand
685 Genomic Sci. **6**:165-173.
686 47. **Taghavi S, Garafola C, Monchy S, Newman L, Hoffman A, Weyens N, Barac T,**
687 **Vangronsveld J, van der Lelie D.** 2009. Genome survey and characterization of
688 endophytic bacteria exhibiting a beneficial effect on growth and development of poplar
689 trees. Appl. Environ. Microbiol. **75**:748-757.
690 48. **Whitfield C.** 2006. Biosynthesis and assembly of capsular polysaccharides in
691 *Escherichia coli*. Annu. Rev. Biochem. **75**: 39-68.
692 49. **Reeves PR.** 1994. Biosynthesis and assembly of lipopolysaccharide, p 281-317. *In*
693 Neuberger A, van Deenen LLM (ed.), *Bacterial Cell Wall: New Comprehensive*
694 *Biochemistry*, vol. 27. Elsevier, New York, NY.
695 50. **Shepherd JG, Wang L, Reeves PR.** 2000. Comparison of O-antigen gene clusters of
696 *Escherichia coli* (*Shigella*) Sonnei and *Plesiomonas shigelloides* O17: Sonnei gained its
697 current plasmid-borne O-antigen genes from *P. shigelloides* in a recent event. Infect.
698 Immun. **68**:6056-6061.
699 51. **Liu B, Knirel YA, Feng L, Perepelov AV, Senchenkova SN, Wang Q, Reeves PR,**
700 **Wang L.** 2008. Structure and genetics of *Shigella* O antigens. FEMS Microbiol. Rev.
701 **32**:627-53.
702 52. **Mullane N, O'Gaora P, Nally JE, Iversen C, Whyte P, Wall PG, Fanning S.** 2008.
703 Molecular analysis of the *Enterobacter sakazakii* O-antigen gene locus. Appl. Environ.
704 Microbiol. **74**:3783-3794.
705 53. **Collins RF, Beis K, Dong C, Botting CH, McDonnell C, Ford RC, Clarke BR,**
706 **Whitfield C, Naismith JH.** 2007. The 3D structure of a periplasm-spanning platform
707 required for assembly of group 1 capsular polysaccharides in *Escherichia coli*. Proc. Natl.
708 Acad. Sci. USA. **104**:2390-2395.

709 54. **Jenke-Kodama H, Sandmann A, Müller R, and Dittmann E.** 2005. Evolutionary
710 implications of bacterial polyketide synthases. Mol. Biol. Evol. **22**:2027-2239.
711 55. **Syvanen M.** 2012. Evolutionary implications of horizontal gene transfer. Annu. Rev.
712 Genet. **46**:341-358.
713 56. **Lang AS, Zhaxybayeva O, Beatty JT.** 2012. Gene transfer agents: phage-like
714 elements of genetic exchange. Nat. Rev. Microbiol. **10**:472-482.
715 57. **Aminov RI.** 2011. Horizontal gene exchange in environmental microbiota. Front
716 Microbiol. **2**:158.
717 58. **Wiedenbeck J, Cohan FM.** 2011. Origins of bacterial diversity through horizontal
718 genetic transfer and adaptation to new ecological niches. FEMS Microbiol Rev. **35**:957-
719 976.
720 59. **Regué M, Fabregat C, Viñas M.** 1991. A generalized transducing bacteriophage for
721 *Serratia marcescens*. Res. Microbiol. **142**:23-27.
722 60. **Evans TJ, Crow MA, Williamson NR, Orme W, Thomson NR, Komitopoulou E,**
723 **Salmond GP.** 2010. Characterization of a broad-host-range flagellum-dependent phage
724 that mediates high-efficiency generalized transduction in, and between, *Serratia* and
725 *Pantoea*. Microbiology **156**:240-247.
726 61. **Petty NK, Toribio AL, Goulding D, Foulds I, Thomson N, Dougan G, Salmond GP.**
727 2007. A generalized transducing phage for the murine pathogen *Citrobacter rodentium*.
728 Microbiology **153**:2984-2988.
729 62. **Blower TR, Evans TJ, Przybilski R, Fineran PC, Salmond GP.** 2012. Viral evasion
730 of a bacterial suicide system by RNA-based molecular mimicry enables infectious altruism.
731 PLoS Genet **8**:e1003023.
732 63. **Cerquetti MC, Hooke AM.** 1993. Vi I typing phage for generalized transduction of
733 *Salmonella typhi*. J. Bacteriol. **175**:5294-5296.

64. **Weinbauer MG, Rassoulzadegan F.** 2004. Are viruses driving microbial diversification and diversity? Environ. Microbiol. **6**:1-11.

65. **Bailly-Bechet M, Vergassola M, Rocha E.** 2007. Causes for the intriguing presence of tRNAs in phages. Genome Res. **17**:1486-1495.

66. **Enav H, Béjà O, Mandel-Gutfreund Y.** 2012. Cyanophage tRNAs may have a role in cross-infectivity of oceanic *Prochlorococcus* and *Synechococcus* hosts. ISME J. **6**:619-628.

67. **Łobocka MB, Rose DJ, Plunkett G 3rd, Rusin M, Samojedny A, Lehnherr H, Yarmolinsky MB, Blattner FR.** 2004. Genome of bacteriophage P1. J. Bacteriol. **186**:7032-68.

68. **Wu LT, Chang SY, Yen MR, Yang TC, Tseng YH.** 2007. Characterization of extended-host-range pseudo-T-even bacteriophage Kpp95 isolated on *Klebsiella pneumoniae*. Appl. Environ. Microbiol. **73**:2532-2540.

69. **Walter M, Fiedler C, Grassl R, Biebl M, Rachel R, Hermo-Parrado XL, Llamas-Saiz AL, Seckler R, Miller S, van Raaij MJ.** 2008. Structure of the receptor-binding protein of bacteriophage det7: a podoviral tail spike in a myovirus. Virology **82**:2265-2273.

70. **Suzuki H, Yamada S, Toyama Y, Takeda S.** 2010. The C-terminal domain is sufficient for host-binding activity of the Mu phage tail-spike protein. Biochim. Biophys. Acta **1804**:1738-1742.

71. **Labrie SJ, Samson JE, Moineau S.** 2010. Bacteriophage resistance mechanisms. Nat. Rev. Microbiol. **8**:317-327.

72. **Blower TR, Short FL, Rao F, Mizuguchi K, Pei XY, Fineran PC, Luisi BF, Salmond GP**. 2012. Identification and classification of bacterial Type III toxin-antitoxin systems encoded in chromosomal and plasmid genomes. Nucleic Acids Res. **40**:6158-6173.

73. **Leplae R, Geeraerts D, Hallez R, Guglielmini J, Drèze P, Van Melderen L.** 2011. Diversity of bacterial type II toxin-antitoxin systems: a comprehensive search and functional analysis of novel families. Nucleic Acids Res. **39**:5513-5525.

74. **Hsu CR, Lin TL, Pan YJ, Hsieh PF, Wang JT.** 2013. Isolation of a bacteriophage specific for a new capsular type of *Klebsiella pneumoniae* and characterization of its polysaccharide depolymerase. PLoS One **8**:e70092.

75. **Frazer KA, Pachter L, Poliakov A, Rubin EM, Dubchak I.** 2004. VISTA: computational tools for comparative genomics. Nucleic Acids Res. **32**:W273-9.

76. **Yang YJ, Wu PJ, Livermore DM.** 1990. Biochemical characterization of a beta-lactamase that hydrolyzes penems and carbapenems from two *Serratia marcescens* isolates. Antimicrob. Agents Chemother. **34**:755-758.

782 **Table 1: φMAM1 host range**

Strain	Relevant characteristics	Source or reference	EOP[a]	Morphology	Average plaque size (mm)[d]
Serratia plymuthica A153	Rhizosphere isolate, oocydin A$^+$	19	1	Clear	1.5
Serratia marcescens 1695	Clinical isolate, non-pigmented	42	-[b]	Turbid	-
S. marcescens 0006	Environmental isolate, non-pigmented	42	0.6[c]	Turbid	0.1
S. marcescens 1047	Clinical isolate, non-pigmented	42	0.5[c]	Turbid	0.3
S. marcescens 0026	Environmental isolate, non-pigmented	42	1.2	Clear	0.7
S. marcescens 3078	Clinical isolate, pigmented	42	1.2	Clear	1
S. marcescens 0038	Environmental isolate, pigmented	42	0.3	Clear	1
S. marcescens 3127	Clinical isolate, non-pigmented	42	0.3	Turbid	0.5
S. marcescens 0035	Environmental isolate, pigmented	42	0.1	Clear	0.5
S. marcescens 12	Clinical isolate, non-pigmented	42	0.3	Clear	0.1
S. marcescens 0040	Environmental isolate, pigmented	42	1.4	Clear	1.5
S. marcescens 2595	Clinical isolate, non-pigmented	42	-[b]	Turbid	-
S. marcescens 3127	Clinical isolate, pigmented	42	0.6	Clear	1
S. marcescens 3078V	Spontaneous non-pigmented variant of *Sma* 3078	42	0.9	Turbid	0.8
S. marcescens ATCC 274	Clinical isolate, pigmented	66	0.5	Clear	0.5
S. marcescens S6	Clinical isolate, non-pigmented	76	0.6	Turbid	0.8
S. marcescens 365	Lab stock, pigmented	L. Debarbieux	6.1×10^{-3}	Clear	0.1
S. marcescens 2170	Lab stock, pigmented	T. Watanabe	0.9	Clear	1
Kluyvera cryorescens 2Kr27	Rhizosphere isolate	39	0.4	Clear	0.3

783 [a]EOP was determined by dividing the phage titre of the φMAM1-sensitive strain by that of the wild type
784 reference strain, *Serratia plymuthica* A153.

785 [b]No plaques observed. Adsorption assays confirmed that φMAM1 adsorbs to *Sma* 1695 and *Sma* 2595.

786 [c]No phage plaques were observed at 30 ºC. Phage plaques arose at 37 ºC in *Sma* 0006 and *Sma* 1047.

787 [d]0.35% (w/v) LB-agar lawns.

788

789

790

791

792

793

794

Table 2: Frequency of transduction of φMAM1

Number of A153 cells	m.o.i.	Transduction efficiency[a,b]	Standard deviation[b]
1×10^{10}	10	$< 1.0 \times 10^{-11}$	-
	1	3.4×10^{-7}	4.1×10^{-8}
	0.1	2.7×10^{-6}	2.5×10^{-7}
	0.01	3.3×10^{-6}	6.7×10^{-7}
1×10^{9}	10	$< 1.0 \times 10^{-10}$	-
	1	3.0×10^{-7}	1.8×10^{-8}
	0.1	4.5×10^{-6}	3.0×10^{-7}
	0.01	5.8×10^{-6}	9.7×10^{-7}
1×10^{8}	10	$< 1.0 \times 10^{-9}$	-
	1	2.8×10^{-7}	5.9×10^{-8}
	0.1	7.4×10^{-6}	1.2×10^{-6}
	0.01	6.8×10^{-6}	0.9×10^{-6}

[a]Efficiency of transduction, defined as the number of transductants per p.f.u. obtained carrying the *oocJ*::Tn-KRCPN1 marker in the A153 recipient.

[b]Mean and standard deviation of three independent experiments are shown.

Table 3: φMAM1 transduction efficiency of different markers within *Serratia plymuthica* A153, *Serratia marcescens* 12 and *Kluyvera cryorescens* 2Kr27.

Donor strain	Relevant marker/plasmid	Recipient strain	Phenotype	Transduction efficiency[a,b,c]	Standard deviation[b]
Transduction within *Serratia plymuthica* A153					
VN1	*admH*::Km	A153	Antibiotic$^-$	1.8×10^{-6}	2.5×10^{-7}
VN2	*admK*::Km	A153	Antibiotic$^-$	1.1×10^{-6}	1.8×10^{-7}
MMnO13	*oocJ*::Km	A153	Oocydin A$^-$	2.7×10^{-6}	2.5×10^{-7}
MMnO15	*oocU*::Km	A153	Oocydin A$^-$	4.2×10^{-6}	2.3×10^{-7}
OocKmSm	Km,Sm	A153	Oocydin A$^+$	2.1×10^{-7}	3.1×10^{-8}
BcsB	*bcsB*::Sm	A153	Cellulose$^-$	1.3×10^{-6}	1.1×10^{-7}
A153	pECA1039-km3	A153	ToxIN$^+$	2.5×10^{-7}	7.4×10^{-8}
Transduction within *Serratia marcescens* 12					
Sma12I	*luxI*::Km	*Sma* 12	Lactone$^-$	5.3×10^{-6}	1.3×10^{-7}
Dho	*narX*::Km	*Sma* 12	Pyrimidine auxotroph	6.6×10^{-6}	2.7×10^{-7}
Cps	*cps*::km	*Sma* 12	Uracil auxotroph	2.3×10^{-6}	6.9×10^{-8}
Sma12S	*luxS*::Km	*Sma* 12	Autoinducer-2$^-$	7.2×10^{-6}	8.2×10^{-7}
Intergeneric transduction					
A153	pECA1039-km3	2Kr27	ToxIN$^+$	2.7×10^{-7}	2.6×10^{-8}
A153	pECA1039-km3	*Sma* 12	ToxIN$^+$	4.8×10^{-8}	9.6×10^{-9}

[a]The number of transductants showing co-inheritance of the antibiotic resistance and the listed phenotype. Transduction efficiency is expressed as the number of transductants per p.f.u.

[b]Mean and standard deviation of three independent experiments are shown.

[c]Transduction experiments were performed using 10^{10} cells with φMAM1 at an m.o.i. of 0.1.

Table 4: Transduction efficiency of the 77-kbp oocydin A gene cluster by φMAM1.

Donor strain	Relevant Marker	Recipient strain[a]	Antibiotic used[b]	Transduction efficiency	Standard deviation	Restoration of oocydin A production in transductants (%)
OocKmSm	Km,Sm	OocEV	Km	1.2×10^{-6}	4.7×10^{-7}	17.7 ± 4.8
OocKmSm	Km,Sm	OocEV	Sm	2.1×10^{-6}	4.2×10^{-7}	9.5 ± 2.0
OocKmSm	Km,Sm	OocEV	Km,Sm	1.9×10^{-7}	1.7×10^{-8}	100 ± 0

[a]OocEV is a markerless, double in-frame deletion mutant defective in the genes *oocE* and *oocV* (Table A1).

[b]Antibiotic used in the selection plate. Km, kanamycin; Sm, streptomycin.

FIGURE AND FIGURE LEGENDS

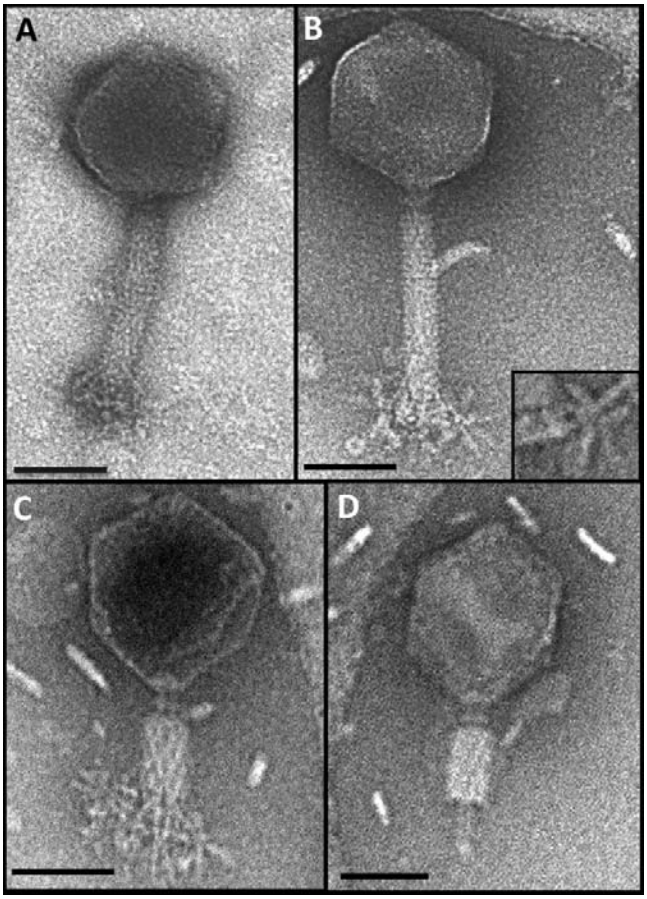

Fig. 1. Transmission electron micrographs of phage φMAM1. A, Intact virion with folded “prong-like” structures. **B**, Intact virion with unfolded “prong-like” structures. A detail of an unfolded structure with the four tail-spike proteins (TSP) attached to the baseplate is also shown. **C**, Intact virion with contracted tail, deformed head and TSP structures. **D**, φMAM1 phage particle lacking the adsorption structures and with the central tube exposed. φMAM1 particles were stained with uranyl acetate (A) or ammonium tungstate (B-D) as described in materials and methods. Bars, 50 nm.

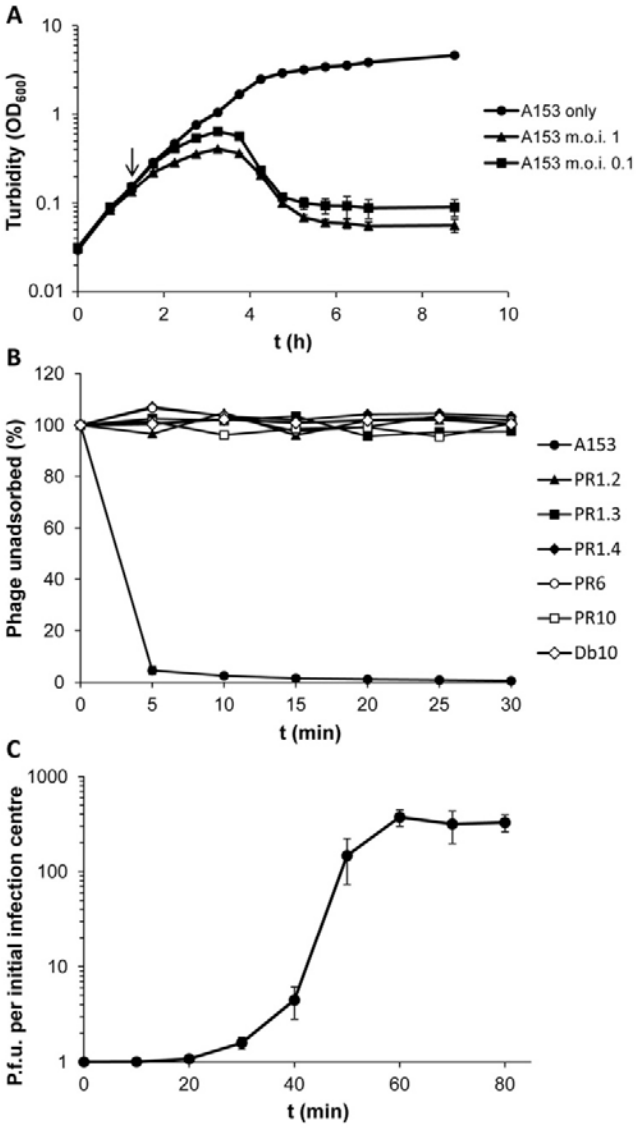

865

866 **Fig 2. Biological characterization of φMAM1. A**, *Serratia plymuthica* A153 growth
867 curves in the presence and absence of φMAM1. Phage was added at an m.o.i. of 0.1 and
868 1 to A153 in the early exponential phase of growth as described Petty *et al*., (25). The
869 arrow indicates the point of addition of φMAM1. ***B, Adsorption of*** φMAM1 to A153 and
870 A153 phage resistant (PR) mutants. The φMAM1 insensitive strain *Serratia marcescens*
871 Db10 was used as negative control for the adsorption. Description of the strains and the
872 location of the transposon insertion points are shown in Table A1 and Fig. A5,
873 respectively. **C**, One-step growth curve of φMAM1. In all cases, *error bars* represent the
874 *standard deviations (n=3).*

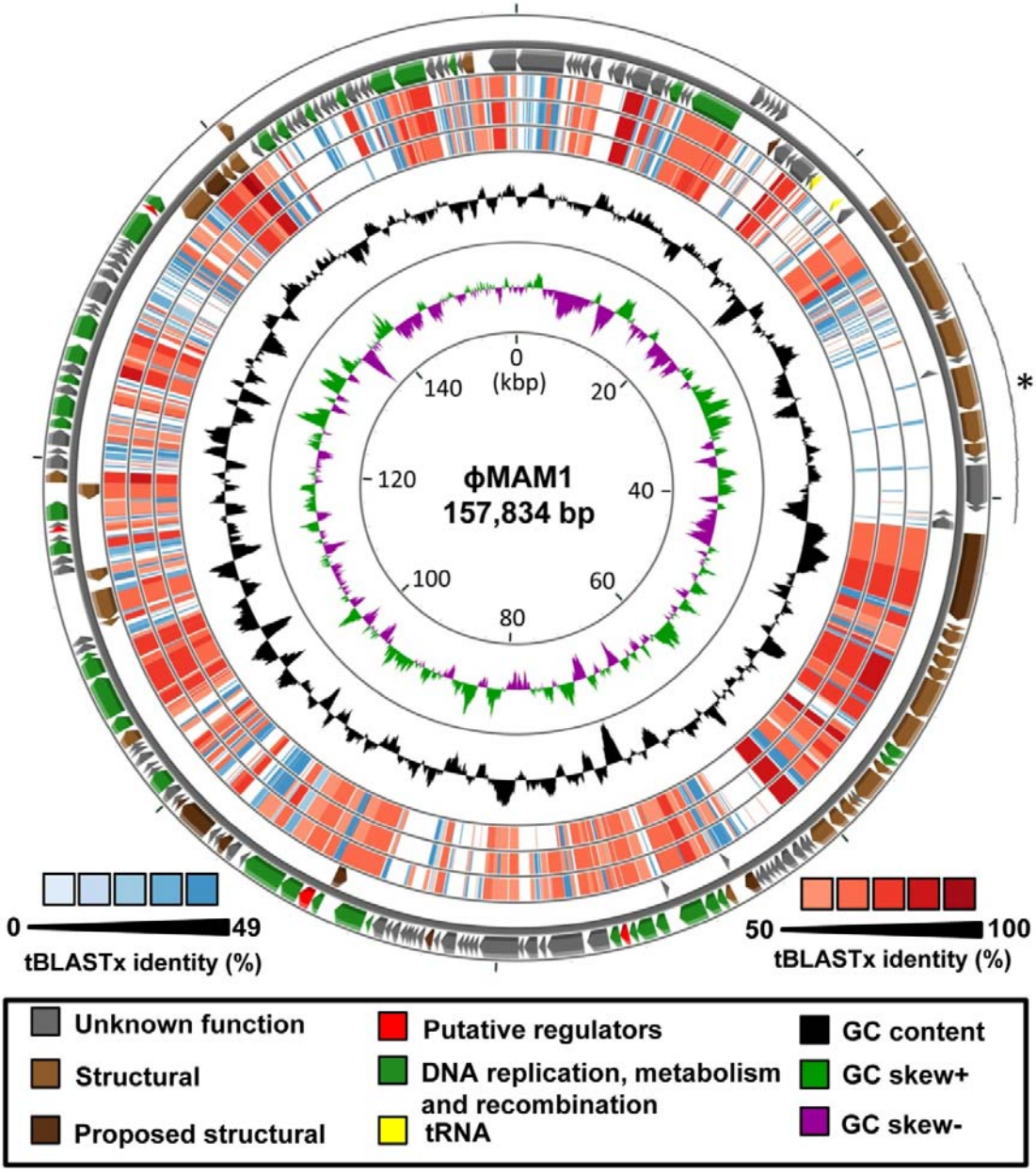

875

876 **Fig. 3: Genome map of phage φMAM1.** The physical locations by strand of all ORFs are
877 shown on the outer ring. Colour code representing the functional category of each gene is
878 given where possible. The proposed structural genes (dark brown) are based on previous
879 mass spectrometry analyses (11,32). The region encoding the host-recognition
880 determinants, the tail spike proteins, is indicated with an asterisk. The three bluish and
881 reddish internal rings represent the tBLASTx results against the Vil-like phages Vi01 (outer
882 ring), φSboM-AG3 (middle ring) and LIMEstone1 (inner ring). GC content and GC skew

analysis are also shown. The genome map was generated using the CGView Comparison Tool (27).

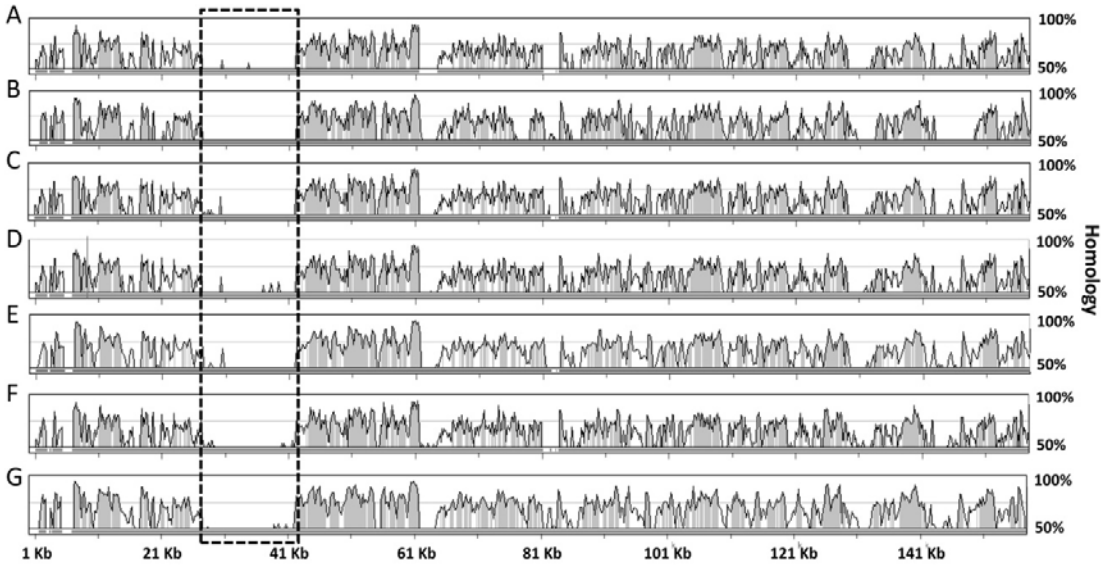

Fig. 4. DNA homology between the genome of φMAM1 and the genomes of seven sequenced Vil-like phages. The alignments represent the percentage of DNA homology between the genome of φMAM1 and those of PhaxI (**A**; 37), LIMEstone1 (**B**; 11), CBA120 (**C**; 36), φSH19 (**D**; 33), SFP10 (**E**; 34), Vi01 (**F**; 32), and φSboM-AG3 (**G**; 35). The regions encoding the host-recognition determinants, the tail spike proteins, are highlighted. Alignments were performed using wgVISTA (75).

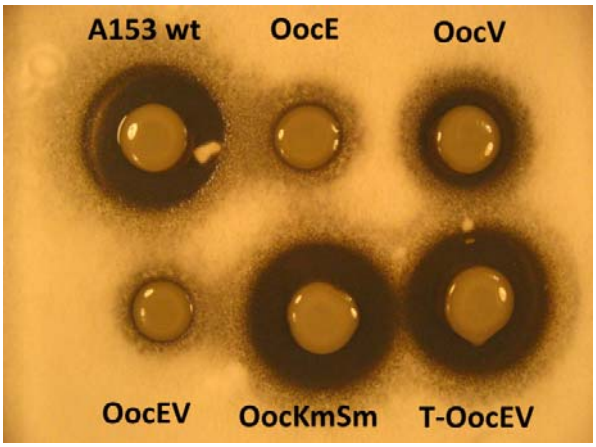

Fig. 5. Mobilization of the oocydin A gene cluster into the non-producing *Serratia plymuthica* A153 OocEV mutant through transduction mediated by phage φMAM1. Production of oocydin A, shown as the ability of inhibiting the growth of the plant pathogenic fungi *Verticillium dahliae*, in several A153 derivative strains. The bioassays were performed as described previously (30). The assays were repeated at least five times, and representative results are shown. Bacterial strains used are listed in Table A1.